This article has been accepted for publication in a future issue of this journal, but has not been fully edited. Content may change prior to final publication. Citation information: DOI 10.1109/TNB.2016.2620439, IEEE Transactions on NanoBioscience

Propagation Modeling and Analysis of Molecular Motors in Molecular Communication

Youssef Chahibi, *Student Member, IEEE,* Ian F. Akyildiz, *Fellow, IEEE,* and Ilangko Balasingham, *Senior Member, IEEE*

***Abstract*—Molecular motor networks (MMNs) are networks constructed from molecular motors to enable nanomachines to perform coordinated tasks of sensing, computing, and actuation at the nano- and micro- scales. Living cells are naturally enabled with this same mechanism to establish point-to-point communication between different locations inside the cell. Similar to a railway system, the cytoplasm contains an intricate infrastructure of tracks, named microtubules, interconnecting different internal components of the cell. Motor proteins, such as kinesin and dynein, are able to travel along these tracks directionally, carrying with them large molecules that would otherwise be unreliably transported across the cytoplasm using free diffusion. Molecular communication has been previously proposed for the design and study of MMNs. However, the topological aspects of MMNs, including the effects of branches, have been ignored in the existing studies. In this paper, a physical end-to-end model for MMNs is developed, considering the location of the transmitter node, the network topology, and the receiver nodes. The end-to-end gain and group delay are considered as the performance measures, and analytical expressions for them are derived. The analytical model is validated by Monte-Carlo simulations and the performance of MMNs is analyzed numerically. It is shown that, depending on their nature and position, MMN nodes create impedance effects that are critical for the overall performance. This model could be applied to assist the design of artificial MMNs and to study cargo transport in neurofilaments to elucidate brain diseases related to microtubule jamming.**

***Index Terms*—Nanonetworks, molecular motors, molecular communication, wave propagation, channel modeling.**

I. Introduction

Molecular motors are biological nanomachines that enable living organisms to perform efficient mechanical work, including muscle contraction and the intracellular cargo transport. In particular, kinesin and dynein are two important motor proteins enabling the intracellular cargo transport towards and away from the cell nucleus, respectively. They convert energy in the form of adenosine triphosphate (ATP) to transport large molecules inside a cell between different organelles and vesicles.

Molecular motor communication (MMC) is a walkway-based molecular communication (MC) mechanism. MMC underlies intercellular neuron communication [18] by transporting large molecules along the axons of a neuron cell, as well as intracellular communication between the nucleus and the organelles of a cell. MMC has several advantages over other MC physical solutions. Diffusion-based molecular communication [23] is not fast enough to transport molecules over large distances ($\gg 1\ \mu m$). In addition, diffusion-based molecular communication cannot happen against the concentration gradient in the medium. Similarly, flow-based communication cannot occur against the flow direction. MMC does not have this limitation. In fact, molecular motors can transport molecules in non-equilibrium mediums, regardless of the concentration gradient, by using chemical energy (e.g., in the form of ATP) to produce a mechanical movement in a similar way to a car engine. The ability to control the motion of molecular motors using molecular switches [5] makes MMC a promising solution to realize nanonetworks [1].

Unlike macro-scale motors, molecular motors are highly stochastic in nature. MMC has been conceptually considered as a molecular communication mechanism in [27]. In [19], the noise effects of molecular motors traveling along microtubular tracks have been simulated using a one-dimensional random walker with drift. In [22], MMC using microtubular transport over kinesin-coated surfaces has been simulated as a random walker with drift on a two-dimensional geometry. These works are based on mobility models that assume empirically-measured drift velocity and diffusivity. In reality, the drift velocity and diffusivity are highly coupled. Moreover, molecular motors often detach from their track. The paper in [10] provides experimental results for the transport of microtubules on kinetic-coated surfaces, demonstrating the feasibility of MMC. The paper also utilizes DNA hybridization to create a MC addressing scheme. The paper in [13] uses Monte-Carlo methods to simulate molecular motor transport on cytoskeletal filaments. The paper has the advantage of taking into account the mutual exclusion of molecular motors, but considers only two molecular motor states (forward motion, and detachment state). Several computational models have been proposed to capture this behavior with varying levels of complexity [14] [15].

In this paper, a fully analytical propagation model of the MMC channel is developed and its performance analysis is conducted based on the mobility parameters (backward

Youssef Chahibi and Ian F. Akyildiz are with the Broadband Wireless Networking Laboratory, School of Electrical and Computer Engineering, Georgia Institute of Technology, Atlanta, GA 30332, USA (email: {youssef,ian}@ece.gatech.edu).

Ilangko Balasingham is with the Biomedical Sensor Network Research Group at the Norwegian University of Science and Technology (NTNU), Institute of Mathematics and Electronics, the Intervention Center at the Oslo University Hospital, and the Institute of Clinical Medicine, University of Oslo (email: ilangkob@iet.ntnu.no).

This work was performed at the Norwegian University of Science and Technology (NTNU) during the tenure of a Mobility Scholarship as a part of the project "Medical Sensing, Localization, and Communications using Ultra Wideband Technology (MELODY) II" contract no. 225885/O70 funded by the Research Council of Norway.

motion, forward motion, and detachment) of the molecular motor protein (kinesin and dynein) moving along a bifurcating network of microtubules. The end-to-end gain and group delay in a MMN are derived analytically in the frequency domain. They depend on the MMN topology, the locations of the transmitter and receiver nodes, and the mobility parameters of the molecular motors. In order to verify the analytical model, we compare the model with the results of Markov Chain Monte-Carlo simulations of a molecular motor. Our results could be used for medical applications. For example, molecular motors are involved in several diseases and therapeutic methods. In fact, several brain diseases are associated with jamming in microtubules, which prevents the transport of key proteins needed for the repair of brain cells [9]. Our analytical results could be used to find the molecular properties that cause jamming and diagnose the jamming points in a MMN.

The paper is organized as follows. In Sec. II, the system model is presented, including the network topology and the molecular motor mobility. In Sec. III, the propagation model of molecular motors over a network is explained. In Sec. IV, numerical results stemming from the numerical evaluation of the MMC network are presented, discussed, and compared with the results of Monte-Carlo simulations. Finally, Sec. V concludes the paper.

II. Analysis of Point-to-point Molecular Communication with Molecular Motors

In this section, the topology and elements of a MMN are presented, the mobility of molecular motors on microtubules is described and modeled through a Markov Process, and a Fokker-Planck equation for the probability density function of the presence of a molecular motor on the MMN is provided.

A. Molecular Motor Network Model

Fig. 1 shows the topology of a MMN. The root node of the MMN is the soma. The microtubule tracks may bifurcate, as is the case in neurons [11] and plants [4]. A microtubule is abstracted as a link. The bifurcations are abstracted as nodes. The location of cargo production is abstracted as a transmitter node. The location of cargo absorption is abstracted as a receiver node. The nodes that do not have any children nodes are called terminal modes. An example of cargo is messenger ribonucleic acid (mRNA). The transport of the cargo is carried out by molecular motors which travel along the microtubules. The molecular motors consist of kinesin, which is a motor protein that travels towards the $(+)$ end of the microtubule, and dynein, which travels in the opposite direction towards the $(-)$ end. The cargo can be blocked when it reaches the terminal nodes of the MMN.

The topology of the MMN is assumed to be a binary tree graph, i.e., one node can only have up to two children nodes. This is the case for microtubules in neurons, due to the shape of dendritic trees. The MMN has a finite number of nodes (vertices) N and $N-1$ links (edges). The nodes can be transmitter nodes, branching nodes, or receiver nodes. An example of a binary tree topology with 5 nodes is illustrated in Fig. 2. The node that is the closest to the cell soma is called the root node and has index 1. A conventional indexing scheme is used for any other node. If it is located to the left of its parent k, the index is $2k$, otherwise, the index is $2k+1$. In the figure, the nodes 2, $2k=6$, and $2k+1=7$ are terminal nodes with $k=3$.

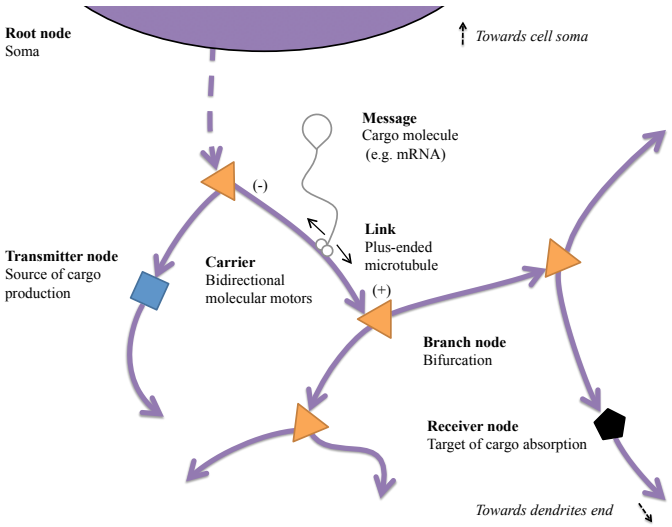

Fig. 1: Molecular motors travel along the cytoskeleton, away from the soma and towards the ends of the dendrites. However, they can also travel in the opposite direction due to their random behavior. Molecular communication is used to abstract the propagation of molecular motors on the cytoskeleton as a communication network.

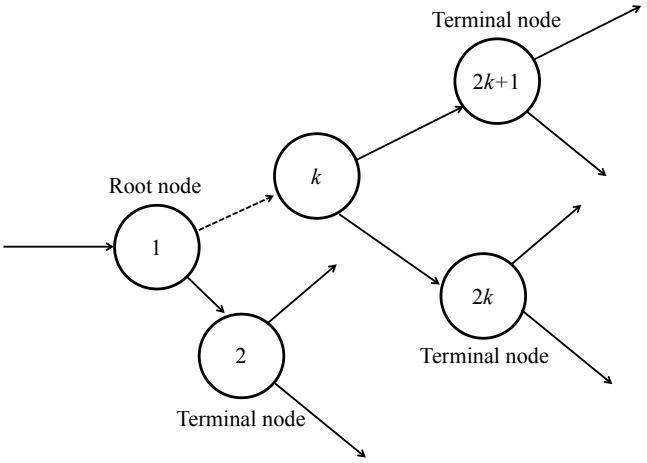

Fig. 2: Illustration of a MMN with a binary tree topology.

B. Molecular Motor Mobility

The mobility model for molecular motors is based on the experimental observations regarding the biophysics of protein transport inside the cell. It has been observed in [21] that molecular motors undergo stochastic transitions between different motion states, namely the backward motion state, the detachment state, and the forward motion state. The molecular

This article has been accepted for publication in a future issue of this journal, but has not been fully edited. Content may change prior to final publication. Citation information: DOI 10.1109/TNB.2016.2620439, IEEE Transactions on NanoBioscience

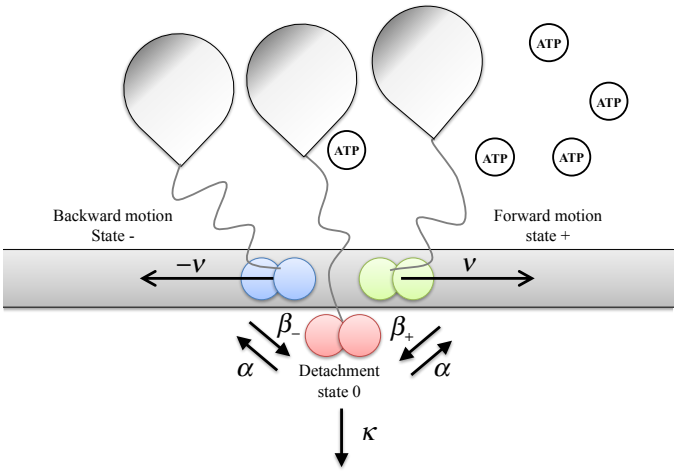

Fig. 3: State representation of molecular motors motion.

motor moves with a velocity $-\nu$ in the backward motion state, with a velocity 0 at the detachment state, and with a velocity ν at the forward motion state. In the detachment state, the molecular motor does not move and may irreversibly detach from the microtubule track at a rate κ, otherwise it returns to one of the two motion states at a rate α.

Fig. 3 shows a molecular motor traveling along a microtubule and carrying a cargo. The mechanical energy of the molecular motor comes from the available chemical energy contained in ATP molecules. As shown in the figure, α is the rate at which the molecular motors moves from a detached state to a backward or forward state. β_+ and β_- is the rate at which the molecular motor move from a forward motion state, or a backward motion state, respectively, to a detached state. We note that a molecular motor cannot directly transition between a forward motion state and a backward motion state [8]. At the detached state, the molecular motor does not move and may either irreversibly detach by the surrounding environment or return to one of the motion states The molecular motor irreversibly detaches from the microtubule when it reaches the end of the microtubules. The transmitter and receiver nodes can be located anywhere in the network.

Mechanochemical studies of motor proteins under different ATP concentrations [25] have shown that their velocity increases with the ATP concentration. It reaches a maximum velocity at saturating levels of ATP. More precisely, the velocity is related to ATP concentration according to Michaelis-Menten kinetics [28]. This model defines a constant K_{ATP}, named Michaelis constant, as the concentration of ATP c_{ATP} at which the velocity is half of ν_{max}. In this paper, we use $\nu_{max} = 0.1\mu s$, which is approximately equal to the velocity observed in experiments [3]. Thus, the velocity ν is a function of the chemical energy as follows [21]

$$\nu = \frac{\nu_{max} c_{ATP}}{c_{ATP} + K_{ATP}}\,. \tag{1}$$

C. Markov Process Model of Molecular Motors

A convenient way to describe the switching of molecular motors between different states is through a Markov process [21]. The kinetics of a molecular motor can then be described as a Markov process with different states (backward motion, detachment, and forward motion). In this section, the Markov process and its set of parameters are described in detail.

A molecular motor can be in the position $X(t) \in \mathbb{R}$ and at the state $S(t) \in (+, -, 0)$. $X(t)$ is a continuous random process defining the coordinate along the microtubule at time t and $S(t)$ is a discrete random process defining the state of the molecular motor at time t. The motion and state dynamics are as follows

- **Backward motion state** $-$: the molecular motor moves in the backward direction of the microtubule with a velocity ν, the molecular motor can go from this state to a detachment state with a rate β_-. Let $h_-(x,t)$ denote the joint probability that $x < X(t) < x + dx$ and $S(t) = -$.
- **Detachment state** 0: The molecular motor is still and detaches from the microtubule. It can disappear at rate κ or go to either the forward motion state or the backward motion state with a rate α. Let $h_0(x,t)$ denote the joint probability that $x < X(t) < x + dx$ and $S(t) = 0$.
- **Forward motion state** $+$: The molecular motor moves in the forward direction of the microtubule with a velocity ν, the molecular motor can go from this state to a detachment state with a rate β_+. Let $h_+(x,t)$ denote the joint probability that $x < X(t) < x + dx$ and $S(t) = +$.

From the Markov process model of molecular motors, we can derive the master equations of the molecular motors which describe the variations over time of the probability density functions $h_-(x,t)$, $h_0(x,t)$, and $h_+(x,t)$.

A molecular motor is in state $-$ at position x and time $t + dt$ either if it was a state $-$ at position $x + \nu dt$ and time t or if it moved to the state $-$ from the other states $m \in \{-, 0, +\}$ and did not move out from the state $-$ and other states $m \in \{-, 0, +\}$. Thanks to the Chapman-Kolmogorov equation applied to a discrete Markov process, this is written as the following

$$\begin{aligned} h_-(x, t+dt) &= h_-(x + \nu dt, t) \\ &\quad + \sum_m \left(P_{(m,-)} h_m(x,t) - P_{(-,m)} h_-(x,t) \right) \end{aligned} \tag{2}$$

where $P_{(m,n)}$ is the probability of moving from the state $m \in \{-, 0, +\}$ to the state $n \in \{-, 0, +\}$ during the time interval $[t, t + dt]$. Similarly, for states $+$ and $-$, we have

$$\begin{aligned} h_+(x, t+dt) &= h_+(x - \nu dt, t) \\ &\quad + \sum_m \left(P_{(m,+)} h_m(x,t) - P_{(+,m)} h_+(x,t) \right) \end{aligned} \tag{3}$$

For the detachment state

$$\begin{aligned} h_0(x, t+dt) &= \\ &\quad + \sum_m \left(P_{(m,0)} h_m(x,t) - P_{(0,m)} h_0(x,t) \right)\,. \end{aligned} \tag{4}$$

By using the definition of the rates α, β_+, β_-, and κ and developing the previous equations to a first-order Taylor approximation with respect to dt, we get the following sys-

tem of master equations which governs the evolution of the probability densities for the states $m \in \{-, 0, +\}$.

$$\frac{\partial h_+(x,t)}{\partial t} = -\nu \frac{\partial h_+(x,t)}{\partial x} - \beta_+ h_+(x,t) + \alpha h_0(x,t) \quad (5)$$

$$\frac{\partial h_-(x,t)}{\partial t} = \nu \frac{\partial h_-(x,t)}{\partial x} - \beta_- h_-(x,t) + \alpha h_0(x,t) \quad (6)$$

$$\frac{\partial h_0(x,t)}{\partial t} = \beta_+ h_+(x,t) + \beta_- h_-(x,t) - (2\alpha + \kappa) h_0(x,t)\,. \quad (7)$$

We note that although the equations in (5) are linear, solving them directly using Fourier analysis leads to intractable solutions due to third degree polynomial equations. The master equation in (5) can be solved stochastically by using the kinetic Monte-Carlo Gillespie algorithm [7] or deterministically by using finite-element methods [12]. Although these methods are accurate, they are computationally expensive. At the expense of a first-order approximation, the quasi-state reduction of the master equation to a one-dimensional Fokker-Planck equation [17] is much more computationally efficient and can be used for accurate mathematical analysis of the MMNs.

D. Fokker-Plank Equation

The one-dimensional Fokker-Planck equation governing the probability density function $h(x,t)$ for the presence of the molecular motor at position x and time t can be found from the aforementioned master equation (5). This is done along the lines with the approaches proposed in [20], [21], [24] and [26]. The difference from the previous work is that we assume that the molecular motor may be irreversibly detached at any time and position along the microtubule independently of the target. We omit the full derivation here due to lengthiness. Basically, the master equation (5) is written in matrix form, projected on the orthogonal space of the matrix, the orthogonal projection is expanded asymptotically. Keeping only the first order terms of the expansion, the orthogonal projection is substituted in the matrix form of the master equation, where the diffusion, drift, and reaction terms are identified. The probability density function $h(x,t)$ for the molecular motor at position x and time t is then found to obey the following Fokker-Planck equation

$$\frac{\partial h(x,t)}{\partial t} = -V \frac{\partial h(x,t)}{\partial x} + D \frac{\partial^2 h(x,t)}{\partial x^2} - \Lambda h(x,t)\,. \quad (8)$$

where

- **The diffusion term** D is expressed as

$$D = \frac{2\nu^2}{\gamma^3 \beta_+^2 \beta_-^2 \alpha^2} \left(\beta_-^2 - 4\alpha^2 + 2\alpha\beta_- + \alpha\beta_+ + \alpha\beta_-\right)\,. \quad (9)$$

  with $\gamma = 1/\beta_+ + 1/\beta_- + 1/\alpha$.
- **The drift term** V is expressed as

$$V = \frac{\nu}{\gamma}\left(\frac{1}{\beta_+} - \frac{1}{\beta_-}\right)\,. \quad (10)$$

- **The reaction term** Λ is expressed as

$$\Lambda = \frac{\kappa}{\gamma\alpha}\,. \quad (11)$$

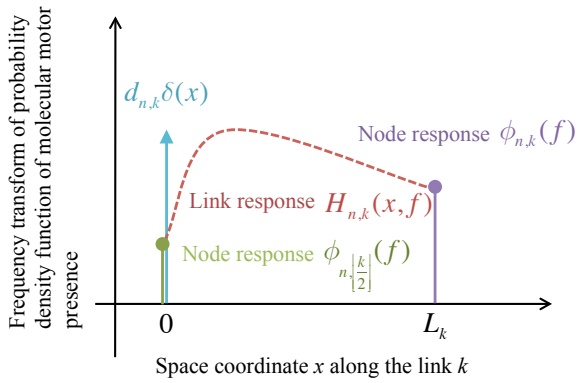

Fig. 4: Link response in a MMN $H_{n,k}(x,f)$, the node response in a MMN $\phi_{n,k}(f)$, and the parent node response $\phi_{n,\lfloor \frac{k}{2} \rfloor}(f)$ in a link k. The x-axis corresponds to the space coordinate x along the link k. The y-axis corresponds to the frequency transform of the probability density function of molecular motor presence.

III. Propagation Analysis in a Molecular Motor Network

We analyze the propagation of one molecular motor along a MMN. The molecular motor is located at the inlet of a link n at the time $t = 0$, and we would like to predict how likely the molecular motor will be at another location of the MMN at some t. The case of multiple transmitters and sinks can be considered by the superposition principle since the system of master equations is linear. The analysis is performed in the frequency domain. In this goal, key quantities involved in the propagation analysis are defined as follows

Definition 1. *The **link response in a MMN** $H_{n,k}(x,f)$ is the Fourier transform of $h_{n,k}(x,t)$, the probability density function, i.e. the characteristic function, for the presence of the molecular motor in the link k at position x and time t given that the molecular motor was located at the inlet of the link n at time $t = 0$. f is the frequency.*

Definition 2. *The **node response in a MMN** $\phi_{n,k}(f)$ is equal to $H_{n,k}(L_k, f)$, where L_k is the length of the link k.*

In Sec. III-A, the link responses in a MMN $H_{n,k}(x,f)$ are found as an expression of the node responses $\phi_{n,\lfloor \frac{k}{2} \rfloor}(x,f)$ and $\phi_{n,k}(f)$ delimiting the links k, as shown in Fig. 4. In Sec. III-B, the node responses in a MMN $\phi_{n,k}(f)$ are found as an expression of the topology and mobility parameters of the MMN. As it will be shown in the derivation, the advantage of this approach is that the link response does not need to be evaluated for the calculation of the node responses, unless it is needed. In fact, given only the length of the links, the link responses can be directly calculated from the node responses.

A. Link Response in a Molecular Motor Network

Here we introduce the procedure for the calculation of a link response $H_{n,k}(x,f)$ in a MMN depending on the node responses $\phi_{n,\lfloor \frac{k}{2} \rfloor}(x,f)$ and $\phi_{n,k}(f)$ delimiting the links k

This article has been accepted for publication in a future issue of this journal, but has not been fully edited. Content may change prior to final publication. Citation information: DOI 10.1109/TNB.2016.2620439, IEEE Transactions on NanoBioscience

and the index of the transmitter node n. After applying the Fourier transform to the Fokker-Planck equation in the time domain derived in (8), the link response in a MMN $H_{n,k}(x,f)$ can be found analytically by solving the following differential equation

$$\left[D\frac{\partial^2}{\partial x^2} - V\frac{\partial}{\partial x} - (2\pi jf + \Lambda)\right] H_{n,k}(x,f) = d_{n,k}\delta(x) \tag{12}$$

where $d_{n,k}$ is the Kronecker symbol (if $n = k$ then $d_{n,k} = 0$, otherwise $d_{n,k} = 1$) and $\delta(\cdot)$ is the Dirac function.

By using standard methods [16], the solution is

$$H_{n,k}(x,f) = H^G_{n,k}(x,f) + H^I_{n,k}(x,f) \tag{13}$$

where $H^G_{n,k}(x,f)$ is the homogeneous function of the equation (12) , and $H^I_{n,k}(x,f)$ is the inhomogeneous solution of the equation (12) satisfying the boundary conditions imposed by $\phi_{n,\lfloor \frac{k}{2} \rfloor}(f)$ at $x = 0$ and $\phi_{n,k}(f)$ at $x = L_k$.

By using a Laplace transform with respect to the spatial coordinate [20], we find that the homogeneous solution $H^G_{n,k}(x,f)$ is expressed as

$$H^G_{n,k}(x,f) = \frac{\psi(x - L_k, f)\psi(x,f)}{DW_k(f)} d_{n,k} \tag{14}$$

where

$$\begin{cases} \psi(x,f) = e^{\mu_1(f)x} - e^{\mu_2(f)x} \\ \mu_1(f) = \frac{V + \sqrt{8j\pi Df + 4D\Lambda + V^2}}{2D} \\ \mu_2(f) = \frac{V - \sqrt{8j\pi Df + 4D\Lambda + V^2}}{2D} \\ W_k(f) = (\mu_2(f) - \mu_1(f))\left(e^{-\mu_1(f)L_k} - e^{-\mu_2(f)L_k}\right) . \end{cases} \tag{15}$$

By using the same method, we find that $H^I_{n,k}(x,f)$ is expressed as follows

$$H^I_{n,k}(x,f) = \phi_{n,\lfloor \frac{k}{2} \rfloor}(f)\frac{\psi(x - L_k, f)}{\psi(-L_k, f)} + \phi_{n,k}(f)\frac{\psi(x,f)}{\psi(L_k,f)} \tag{16}$$

where $\psi(x,f)$ is defined in (15).

Finally, the link response in a MMN is obtained as follows

$$\begin{aligned} H_{n,k}(x,f) = {} & \phi_{n,\lfloor \frac{k}{2} \rfloor}(f)\frac{\psi(x - L_k, f)}{\psi(-L_k, f)} + \phi_{n,k}(f)\frac{\psi(x,f)}{\psi(L_k,f)} \\ & + \frac{\psi(x - L_k, f)\psi(x,f)}{DW_k(f)} d_{k,n} \end{aligned} \tag{17}$$

where $\psi(x,f)$ and $W_k(f)$ are direct expressions of the diffusion term D, the drift term V, and the reaction term Λ of the Fokker-Planck equation in (8).

B. Node Response in a Molecular Motor Network

In this section, a method to determine the node responses $\phi_{n,k}(f)$ in a MMN is proposed, given the topology and geometric properties of the MMN. Based on flux conservation, the analytical expression (18) of node responses in a MMN $\phi_{n,k}(f)$ is obtained. The rest of this section is composed of two parts. First, the problem of deriving the node responses in a MMN $\phi_{n,k}(f)$ is put in matrix form, and second, the matrix form is inverted using an iterative method.

a) Node Responses Matrix Equation: The node response in a MMN matrix equation is obtained by applying the conservation of fluxes at the nodes k. The link inflow and outflow are defined as follows

$$\begin{cases} I_k(f) = -D\frac{\partial H_{n,k}(x,f)}{\partial x}\Big|_{x=0} + VH_{n,k}(0,f) \\ O_k(f) = -D\frac{\partial H_{n,k}(x,f)}{\partial x}\Big|_{x=L_k} + VH_{n,k}(L_k,f) \end{cases} \tag{19}$$

where $I_k(f)$ is the link inflow and $O_k(f)$ is the link outflow. The flux operator $\mathcal{F}\{\cdot\}$ of any function is defined as follows

$$\mathcal{F}\{\cdot\} = \left[-D\frac{\partial}{\partial x} + V\right]\{\cdot\} . \tag{20}$$

Thus $I_k(f) = \mathcal{F}\{H_{n,k}(x,f)\}\,|_{x=0}$ and $O_k(f) = \mathcal{F}\{H_{n,k}(x,f)\}\,|_{x=L_k}$. The flux conversation imposes the following equality

$$O_k(f) = \sum_{m\in\{0,1\}} I_{2k+m}(f) = I_{2k}(f) + I_{2k+1}(f) \tag{21}$$

where $m \in \{0,1\}$ is the relative index of the left and right children links, respectively. Using the definition of flux in (19), the conversation of flux in (21), the definition of the flux operator in (20), and the expression of the link response in a MMN in (17), we obtain an equation that relates the node responses in a MMN as follows

$$\begin{aligned} & \phi_{n,\lfloor \frac{k}{2} \rfloor}(f)\,\mathcal{F}\left\{\frac{\psi(x - L_k, f)}{\psi(-L_k,f)}\right\}\Big|_{x=L_k} \\ & \quad + \phi_{n,k}(f)\,\mathcal{F}\left\{\frac{\psi(x,f)}{\psi(L_k,f)}\right\}\Big|_{x=L_k} \\ & \quad + d_{n,k}\,\mathcal{F}\left\{\frac{\psi(x - L_k, f)\psi(x,f)}{DW_k(f)}\right\}\Big|_{x=L_k} \\ & \quad = \sum_{m\in\{0,1\}} \left(\phi_{n,k}(f)\,\mathcal{F}\left\{\frac{\psi(x - L_{2k+m}, f)}{\psi(-L_{2k+m},f)}\right\}\Big|_{x=0} \right. \\ & \qquad + \phi_{n,2k+m}(f)\,\mathcal{F}\left\{\frac{\psi(x,f)}{\psi(L_k,f)}\right\}\Big|_{x=0} \\ & \qquad \left. + d_{2k+m,n}\,\mathcal{F}\left\{\frac{\psi(x - L_{2k+m}, f)\psi(x,f)}{DW_k(f)}\right\}\Big|_{x=0}\right) . \end{aligned} \tag{22}$$

Reorganizing the terms in (22), the following is obtained

$$\begin{aligned} & \phi_{n,\lfloor \frac{k}{2} \rfloor}(f)g_k(f) + \phi_{n,k}(f)s_k(f) + d_{n,k}r_k \\ & \quad = \sum_{m\in\{0,1\}} [\phi_{n,k}(f)\bar{s}_{2k+m} + \phi_{n,2k+m}(f)\bar{g}_{2k+m} \\ & \qquad + d_{2k+m,n}\bar{r}_k] \end{aligned} \tag{23}$$

where the function $g_k(f)$ is an input transmission coefficient (the ratio of molecules inflowing from the parent node that go past the outlet of the link k), $s_k(f)$ is an output transmission coefficient (the ratio of molecules outflowing from the node that go past the outlet of the link k), $r_k(f)$ is a link transmission coefficient (the ratio of molecules emitted within the link k that go past the outlet of the link k), $\bar{s}_k(f)$ is an input reflection coefficient (the ratio of molecules outflowing from the child node that move to the outlet of the link k), $\bar{g}_k(f)$ is an

This article has been accepted for publication in a future issue of this journal, but has not been fully edited. Content may change prior to final publication. Citation information: DOI 10.1109/TNB.2016.2620439, IEEE Transactions on NanoBioscience

$$\phi_{n,k}(f)=\frac{(-1)^{k'}\hat{q}_{n,1}}{\hat{p}_1(f)}\prod_{j=0}^{k'-1}\frac{g_{\lfloor k.2^{(j-k')}\rfloor}(f)}{\hat{p}_{\lfloor k.2^{(j-k')}\rfloor}(f)}+\sum_{j=0}^{k'-1}(-1)^{k'-j-1}\frac{\hat{q}_{n,\lfloor k.2^{(j-k')}\rfloor}}{\hat{p}_{\lfloor k.2^{(j-k')}\rfloor}(f)}\prod_{r=j+1}^{k'-1}\frac{g_{\lfloor k.2^{(r-k')}\rfloor}(f)}{\hat{p}_{\lfloor k.2^{(r-k')}\rfloor}(f)} \tag{18}$$

output reflection coefficient (the ratio of molecules reflected from the child node that move to the outlet of the link k), and $\bar{r}_k$(f) is a link reflection coefficient (the ratio of molecules emitted within the link k that move the inlet of the link k). The functions $g_k(f)$, $s_k(f)$, $r_k(f)$, $\bar{s}_k(f)$, $\bar{g}_k(f)$, and $\bar{r}_k(f)$ are obtained by identification with (22) as follows

$$\begin{cases} g_k(f)=\mathcal{F}\left\{\frac{\psi(x-L_k,f)}{\psi(-L_k,f)}\right\}\Big|_{x=L_k} \\ s_k(f)=\mathcal{F}\left\{\frac{\psi(x,f)}{\psi(L_k,f)}\right\}\Big|_{x=L_k} \\ r_k(f)=\mathcal{F}\left\{\frac{\psi(x-L_k,f)\psi(x,f)}{DW_k(f)}\right\}\Big|_{x=L_k} \\ \bar{s}_k(f)=\mathcal{F}\left\{\frac{\psi(x-L_k,f)}{\psi(-L_k,f)}\right\}\Big|_{x=0} \\ \bar{g}_k(f)=\mathcal{F}\left\{\frac{\psi(x,f)}{\psi(L_k,f)}\right\}\Big|_{x=0} \\ \bar{r}_k(f)=\mathcal{F}\left\{\frac{\psi(x-L_k,f)\psi(x,f)}{DW_k(f)}\right\}\Big|_{x=0}). \end{cases} \tag{24}$$

Using the equations in (15), $g_k(f)$, $s_k(f)$, $r_k(f)$, $\bar{s}_k(f)$, $\bar{g}_k(f)$ and $\bar{r}_k$ are expressed as a function of the Fokker-Planck diffusion term D, drift term V, reaction term Λ, the link length L_k, and the frequency f as follows

$$\begin{cases} g_k(f)= \\ \quad e^{\frac{L_kV}{2D}}\frac{\sqrt{8i\pi Df+4D\Lambda+V^2}}{2}\mathrm{csch}\left(\frac{L_k\sqrt{8i\pi Df+4D\Lambda+V^2}}{2D}\right) \\ s_k(f)= \\ \quad \frac{V}{2}+\frac{\sqrt{8i\pi Df+4D\Lambda+V^2}}{2}\coth\left(\frac{L_k\sqrt{8i\pi Df+4D\Lambda+V^2}}{2D}\right) \\ r_k=0 \\ \bar{r}_k=-1 \\ \bar{s}_k(f)=-s_k(f)+V \\ \bar{g}_k(f)=-e^{\frac{-VL_k}{D}}g_k(f) \end{cases} \tag{25}$$

where $\mathrm{csch}\,(\cdot)$ is the hyperbolic cosecant function and $\coth(\cdot)$ is the hyperbolic cotangent function.

Therefore, the following linear system of equations is obtained

- If k is a root node

$$\sum_{m\in\{0,1\}}\left(\phi_{n,2k+m}(f)e^{\frac{-VL_{2k+m}}{D}}g_{2k+m}(f)+d_{n,2k+m}\right) +\phi_{n,k}(f)\left(s_k(f)-2V+\sum_{m\in\{0,1\}}s_{2k+m}(f)\right)=0\,. \tag{26}$$

- If k is a terminal node (i.e. the node k does not have any children nodes)

$$\phi_{n,\lfloor\frac{k}{2}\rfloor}(f)g_k(f)+\phi_{n,k}(f)\left(s_k(f)-2V\right)=0\,. \tag{27}$$

- For all other nodes k:

$$\sum_{m\in\{0,1\}}\left(\phi_{n,2k+m}(f)e^{\frac{-VL_{2k+m}}{D}}g_{2k+m}(f)+d_{n,2k+m}\right) +\phi_{n,\lfloor\frac{k}{2}\rfloor}(f)g_k(f) +\phi_{n,k}(f)\left(s_k(f)-2V+\sum_{m\in\{0,1\}}s_{2k+m}(f)\right)=0\,. \tag{28}$$

The linear system of equations composed of (26), (27), and (28) can be written in matrix form as the following

$$\mathbf{A}(f)\mathbf{\Phi}_n(f)=\mathbf{B}_n \tag{29}$$

where $\mathbf{A}(f)=\{a_{k',k}(f);k,k'=1\dots N\}$ is a matrix defined as

- If k is a root node

$$a_{k',k}(f)=-d_{k',k}\left(s_k(f)-2V+\sum_{m\in\{0,1\}}s_{2k+m}(f)\right) -\sum_{m\in\{0,1\}}d_{k',2k+m}e^{\frac{-VL_{2k+m}}{D}}g_{2k+m}(f)\,. \tag{30}$$

- If k is a terminal node

$$a_{k',k}(f)=-d_{k',\lfloor\frac{k}{2}\rfloor}g_k(f)-d_{k',k}\left(s_k(f)-2V\right)\,. \tag{31}$$

- For all other nodes k

$$a_{k',k}(f)=-d_{k',\lfloor\frac{k}{2}\rfloor}g_k(f) -d_{k',k}\left(s_k(f)-2V+\sum_{m\in\{0,1\}}s_{2k+m}(f)\right) -\sum_{m\in\{0,1\}}\left(d_{k',2k+m}e^{\frac{-VL_{2k+m}}{D}}g_{2k+m}(f)\right)\,. \tag{32}$$

$\mathbf{B}_n=\{b_{n,k};k=1\dots N\}^T$ is a vector defined as follows

- If k is a terminal node

$$b_{n,k}=0\,. \tag{33}$$

- For all other nodes k

$$b_{n,k}=\sum_{m\in\{0,1\}}d_{n,2k+m}\,. \tag{34}$$

Therefore $b_{n,k}=1$ if k is the parent node of n, and $b_{n,k}=0$ otherwise since we will have ($n\neq 2k$ and $n\neq 2k+1$).

$\mathbf{\Phi}_n(f)$ is a vector defined as $\mathbf{\Phi}_n(f)=[\phi_{n,k}(f);k=1\dots N]^T$, which are node responses in a MMN for all nodes k, as defined previously in Sec. III-A.

This article has been accepted for publication in a future issue of this journal, but has not been fully edited. Content may change prior to final publication. Citation information: DOI 10.1109/TNB.2016.2620439, IEEE Transactions on NanoBioscience

The matrix $\mathbf{A}(f)$ is nonsingular, since the boundary conditions are well posed. Therefore the node responses in a MMN can be obtained as

$$\mathbf{\Phi}_n(f) = \mathbf{A}^{-1}(f)\mathbf{B}_n \tag{35}$$

where $\mathbf{A}^{-1}(f)$ is the inverse matrix of $\mathbf{A}(f)$, which can be found by Gaussian elimination in $\mathcal{O}\left(N^3\right)$. However, exploiting the structure of the matrix, it can be calculated through an iterative procedure in $\mathcal{O}\left(N\right)$. Since $\mathbf{B}_n$ is a vector consisting of all zeros except the n-th element which is equal to 1. The node responses in a MMN are simply the columns elements of the matrix $\mathbf{A}^{-1}(f)$, i.e.

$$\mathbf{A}^{-1}(f) = [\mathbf{\Phi}_n(f); n = 1 \dots N] \tag{36}$$

which depends only on the topology and geometry of the MMN, as it is explicitly shown through the expression of the coefficients of the matrix $\mathbf{A}(f)$ in (26), (27), and (28).

b) Node Responses Matrix Inversion: The iterative procedure to obtain the MMN matrix $\mathbf{A}^{-1}(f) = [\mathbf{\Phi}_n(f); n = 1 \dots N]$, based on the Molecular Motor Network Model, geometrical properties, and the frequency f is presented here.

Definition 3. *The network-independent coefficient $p_k(f)$ for a non-terminal node k is defined as*

$$p_k(f) = s_k(f) - 2V + \sum_{m\in\{0,1\}} s_{2k+m}(f)\,. \tag{37}$$

Definition 4. *The network-independent source-dependent coefficient $q_{n,k}$ for a non-terminal node k is defined as*

$$q_{n,k} = -\sum_{m\in\{0,1\}} d_{n,2k+m}\,. \tag{38}$$

Corollary 1. *The network-independent source-dependent coefficient $q_{n,k}$ is equal to the following*

$$q_{n,k} = -d_{\lfloor \frac{n}{2} \rfloor,k}\,. \tag{39}$$

Definition 5. *The network-dependent coefficient $\hat{p}_k(f)$ for a non-terminal node k is defined recursively as*

$$\hat{p}_k(f) = p_k(f) - \sum_{m\in\{0,1\}} \frac{g_{2k+m}(f)\bar{g}_{2k+m}(f)}{\hat{p}_{2k+m}(f)} \tag{40}$$

where $g_{2k+m}(f)$ and $\bar{g}_{2k+m}(f)$ are defined in (25)*.*

Definition 6. *The network-dependent coefficient $\hat{q}_{n,k}$ for a non-terminal node k is defined recursively as*

$$\hat{q}_{n,k} = q_{n,k} - \sum_{m\in\{0,1\}} \frac{\bar{g}_{2k+m}}{\hat{p}_{2k+m}(f)}\hat{q}_{n,2k+m} \tag{41}$$

where $\hat{p}_{2k+m}(f)$ is defined in (40)*.*

Theorem 1. *The node responses in a MMN $\phi_{n,\lfloor \frac{k}{2} \rfloor}(f)$ and $\phi_{n,k}(f)$ are governed by the following equation*

$$\phi_{n,\lfloor \frac{k}{2} \rfloor}(f)g_k(f) + \phi_{n,k}(f)\hat{p}_k(f) = \hat{q}_{n,k} \tag{42}$$

Proof. (42) is proved by backward induction [2], starting from the terminal nodes. Let k be a terminal node. Terminal nodes have open children nodes, which are negligible. Therefore (40) $\hat{q}_{n,k} = q_{n,k}$ and $\hat{p}_k(f) = 0$ for k. Hence, using the definitions in (37) and (38), (27) becomes

$$\phi_{n,\lfloor \frac{k}{2} \rfloor}(f)g_k(f) + \phi_{n,k}(f)\hat{p}_k(f) = \hat{q}_{n,k} \tag{43}$$

which proves (42) for the terminal node k. Let k be now a non-terminal node. Let us assume that (42) holds true for its two children nodes $2k+m$ with $m \in \{0,1\}$, i.e.

$$\phi_{n,2k+m}(f) = \frac{\hat{q}_{n,2k+m} - \phi_{n,k}(f)g_{2k+m}(f)}{\hat{p}_{2k+m}(f)} \tag{44}$$

for $m \in \{0,1\}$. Using the definitions (37) and (38), (28) becomes

$$\sum_{m\in\{0,1\}} (\phi_{n,2k+m}(f)\bar{g}_{2k+m}(f)) + \phi_{n,\lfloor \frac{k}{2} \rfloor}(f)g_k(f) + \phi_{n,k}(f)p_k(f) = q_{n,k}\,. \tag{45}$$

Plugging (44) into the previous equation, the following is obtained

$$\sum_{m\in\{0,1\}} \left(\left(\frac{\hat{q}_{n,2k+m} - \phi_{n,k}(f)g_{2k+m}(f)}{\hat{p}_{2k+m}(f)} \right) \bar{g}_{2k+m}(f) \right) + \phi_{n,\lfloor \frac{k}{2} \rfloor}(f)g_k(f) + \phi_{n,k}(f)p_k(f) = q_{n,k}\,. \tag{46}$$

Expanding the equation, and factorizing the terms with $\phi_{n,k}(f)$, the following is obtained

$$\begin{aligned} &\phi_{n,\lfloor \frac{k}{2} \rfloor}(f)g_k(f) \\ &+ \phi_{n,k}(f)\left(p_k(f) - \sum_{m\in\{0,1\}} \frac{g_{2k+m}(f)\bar{g}_{2k+m}(f)}{\hat{p}_{2k+m}(f)} \right) \\ &= \left(q_{n,k} - \sum_{m\in\{0,1\}} \frac{\bar{g}_{2k+m}(f)}{\hat{p}_{2k+m}(f)}\hat{q}_{n,2k+m} \right)\,. \end{aligned} \tag{47}$$

Finally, by using the definitions in (40) and (6) in the previous equations, the following is obtained

$$\phi_{n,\lfloor \frac{k}{2} \rfloor}(f)g_k(f) + \phi_{n,k}(f)\hat{p}_k(f) = \hat{q}_{n,k} \tag{48}$$

which the relationship (42) for the non-terminal node k, and hence, by backward induction, for all nodes k, including the root node $k = 1$ for which $\phi_{n,\lfloor \frac{k}{2} \rfloor} = 0$ due to the boundary conditions. □

Corollary 2. *The root node response in a MMN $\phi_{n,1}(f)$ is an expression of the network-dependent coefficient $\hat{p}_1(f)$ and the network-dependent source-dependent coefficient $\hat{q}_{n,1}$ as follows*

$$\phi_{n,1}(f) = \frac{\hat{q}_{n,1}}{\hat{p}_1(f)}\,. \tag{49}$$

Theorem 2. *The node responses in a MMN $\phi_{n,k}(f)$ are expressed as a function of the index of the transmitter node n, the network topology, the molecular motor mobility, and the network geometrical parameters. The expression is given in* (18) *where $k' = \lfloor \log_2(k) \rfloor$, and* (40) *and $\hat{q}_{n,k}(f)$ and $\hat{p}_k(f)$ are defined in* (40) *and* (6)*, respectively.*

Proof. This theorem stems from the recursive relationship defined in (44), and can be proven by reverse induction, as

This article has been accepted for publication in a future issue of this journal, but has not been fully edited. Content may change prior to final publication. Citation information: DOI 10.1109/TNB.2016.2620439, IEEE Transactions on NanoBioscience

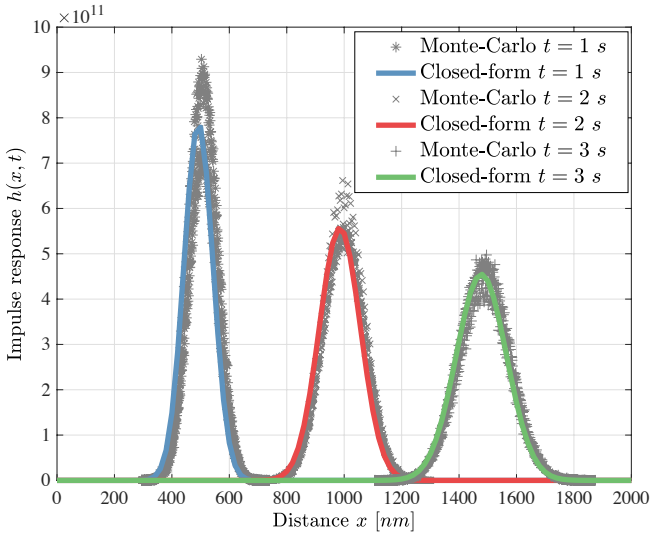

Fig. 5: Comparison between the closed-form channel probability of presence expression and Markov chain Monte-Carlo simulations of the molecular motors motion.

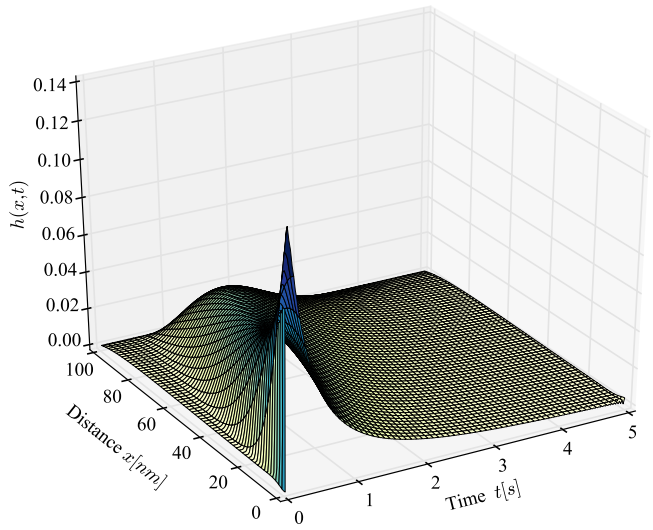

Fig. 6: Evolution of the link response in a MMN within a link separating two nodes. Molecular motors propagate in a wave-like fashion with significant dispersion. In this evaluated scenario, the signal travels over a 100 nm within one second.

it was done for Theorem 1. Using the recursive relationship, a mathematical sequence can be defined with the root node response in a MMN expressed in (18) as the first term of the sequence. □

IV. Numerical Results

A. Monte-Carlo Simulation

Fig. 5 compares the probability density function $h(x,t)$ for the presence of the molecular motor at position x and time t with the histogram of the position of a molecular motor. The simulation environment is based on the Markov Chain Monte-Carlo [6] method, where a number of molecular motors N_m is placed at the initial coordinate $x = 0$, and the motion of each molecular motor is dictated by a coin toss according to the transition diagram shown in Fig. 3. Depending on this random outcome, the molecular motor either moves backward by a distance $-\nu dt$, forward by a distance νdt, or remains in a still position, where dt is the time increment of the simulation. The coin tossing is repeated until the end of the desired simulation time.

Finally, the probability of presence is estimated by evaluating the histogram of the positions of the N_m molecular motors, with a spatial averaging distance dx, and compared with the analytical solution of the Fokker-Planck equation. The closed-form and simulated probabilities of presence match favorably. We notice that contrary to diffusion transport, the noise seems to reduce as the distance increases, and that the noise remains very high compared with the high number of molecular motors N_m on which the results have been averaged.

B. Link Responses in a Molecular Motor Network

As a numerical evaluation, a network topology with 8 nodes has been simulated with the parameters listed in Table I, which are homogeneous for all links.

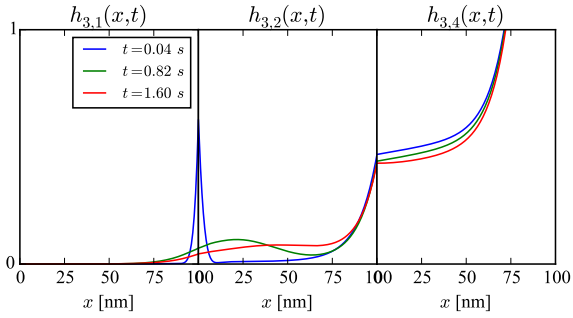

Fig. 7: The link response in a MMN evolution within three connected links at three different time steps $t = 0.04$ s, $t = 0.82$ s, and $t = 1.60$ s, with a transmission from the node 1. The signal is continuous in the bifurcation points but can change drastically over one link. In this evaluated scenario, the signal propagation is clearly favored towards the direction of the drift, away from the root node, where the signal is heavily attenuated.

Fig. 6 shows the probability density function $h(x,t)$ for the presence of the molecular motor at position x and time t in a link separating two nodes. We observe that molecular motors propagate in a wave-like fashion with significant dispersion. In this scenario, the signal travels over a 100 nm within one second.

Fig. 7 shows for the probability density functions $h_{n,k}(x,t)$ for the presence of the molecular motor at position x and time t within three connected links, at three different time steps $t = 0.04$ s, $t = 0.82$ s, and $t = 1.60$ s, with a transmission from the node 3. The signal is continuous in the bifurcation points but can change drastically over one link. In this scenario, the signal propagation is clearly favored towards the direction of the drift, away from the root node, where the signal is quickly

This article has been accepted for publication in a future issue of this journal, but has not been fully edited. Content may change prior to final publication. Citation information: DOI 10.1109/TNB.2016.2620439, IEEE Transactions on NanoBioscience

TABLE I: Numerical values of the molecular motor model.

Parameter	Value
Forward motion rate β_+	0.1 s^{-1}
Backward motion rate β_-	0.5 s^{-1}
Detachment rate α	0.5 s^{-1}
Absorption rate κ	$5\ ms^{-1}$
Speed ν_{max}	0.1 μms^{-1}
ATP concentration c_{ATP}	40 μM
ATP saturation constant K_{ATP}	79.23 μM
Number of molecular motors N_m	30,000
Spatial averaging distance dx	0.045 nm
Link length L_k	300 nm

attenuated.

C. Node Responses in a Molecular Motor Network

The node responses in a MMN have been numerically evaluated, with a transmitter node at the first bifurcation in Fig. 8 and a transmitter node at the second bifurcation in Fig. 8. The gain of the node responses in a MMN is shown in the left part of the figures Fig. 8a and Fig. 9a. The gain of a node response is denoted by $|\phi_{n,k}(f)|$.

The gain of a node response indicates how the signal is attenuated between the transmitter node and the receiver node. We notice in the figures that the gain almost follows a power-law, since the gain is almost linear with respect to the frequency in the log-scale. Also, the steepness of the gain of the node responses increases as the receiver nodes is farther from the transmitter node. In Fig. 8, the transmitter node is far from the terminal nodes, which makes the molecular motor less likely to irreversibly detach from the network. In Fig. 8, the transmitter node is a terminal node, which highly increases the attenuation of the signal. Also, some molecular motors manage to travel to the parallel branch through backward motion.

The group delay is denoted of a node is denoted $\tau_{n,k}(f)$, which is defined as

$$\tau_{n,k}(f) = -\frac{1}{2\pi}\frac{d\angle\phi_{n,k}(f)}{df} \tag{50}$$

where $\angle\phi_{n,k}(f)$ is the phase of the node response $\phi_{n,k}(f)$. The group delay indicates how long a pulse centered around a frequency f is delayed. It is desirable in a communication system to have a constant group delay across the frequencies. We see in Fig. 8b and Fig. 9b, that the group delay drops sharply as the frequency increases. The largest group delay distortion is suffered in the low frequencies. In addition, the group delay is non-linear. This makes time distortion an important challenge in MMC. We observe in both figures that the further the receiver nodes are from the transmitter node, the higher the peak group delay is.

It is clear that the boundary conditions and topology heavily affect the performance of the network. The group delay of the node responses in a MMN is shown in the right part of the figures Fig. 8 and Fig. 9.

V. Conclusion

Molecular motor communication outperforms other classes of molecular communication such as diffusion-based and flow-based communication, which makes it a suitable candidate for designing bio-inspired nanonetworks. In this paper, the propagation of molecular motors along a complex molecular motor nanonetwork (MMN) is predicted analytically based on the location of the transmitter, the mobility properties of the molecular motor, and the topology of the network. The MMN is composed of nodes which can be transmitting, receiving, or idle. The nodes are interconnected with links composed of microtubules. The propagation modeling is solved in the frequency domain. The node responses and link responses are expressed analytically. It is found that the node response in a MMN can be calculated independently of the space dimension, and that the link response is expressed as a function of the two node responses that delimit the link.

The purpose of the paper is to model the propagation channel of molecular motors in a complex network topology carrying a large molecular cargo. An example of such cargo is mRNA which can carry a long sequence of information. Compared with the existing work, the approach undertaken in this paper is completely analytical which simplifies the study of this system. This approach can also be used to study other networks such as microfluidic channels with bifurcations.

The results have been validated by comparison with Monte-Carlo simulations in the time domain. Using numerical evaluations of the model, it is shown that the position of the transmitter node, the mobility properties and topology of the MMN are all critical parameters that affect the node and link responses. Also, it was observed that a transmitter node not only affects the propagation in the children nodes, but also the propagation in the parent nodes which goes against the direction of propagation and in the parallel nodes. In comparison with transmission line network for electromagnetic propagation, MMNs are asymmetrical due to the propagation direction bias of molecular motors. This model can enable the study of other aspects of molecular motors such as energy consumption, noise, information-theoretical capacity, and modulation schemes.

Acknowledgment

The authors would like to thank Pr. Ozgur B. Akan for his valuable remarks that have helped a great deal to improve the quality of the paper.

References

[1] I. F. Akyildiz, J. M. Jornet, and M. Pierobon, "Nanonetworks: A new frontier in communications," *Communications of the ACMs*, vol. 54, no. 11, pp. 84–89, November 2011.

[2] K. G. Binmore, *Mathematical Analysis: a straightforward approach*. Cambridge University Press, 1982.

[3] S. M. Block, L. S. Goldstein, and B. J. Schnapp, "Bead movement by single kinesin molecules studied with optical tweezers," *Nature*, 1990.

[4] J. Chan, A. Sambade, G. Calder, and C. Lloyd, "Arabidopsis cortical microtubules are initiated along, as well as branching from, existing microtubules," *The Plant Cell*, vol. 21, no. 8, pp. 2298–2306, 2009.

[5] J. C. Cochran, Y. C. Zhao, D. E. Wilcox, and F. J. Kull, "A metal switch for controlling the activity of molecular motor proteins," *Nature structural & molecular biology*, vol. 19, no. 1, pp. 122–127, 2012.

This article has been accepted for publication in a future issue of this journal, but has not been fully edited. Content may change prior to final publication. Citation information: DOI 10.1109/TNB.2016.2620439, IEEE Transactions on NanoBioscience

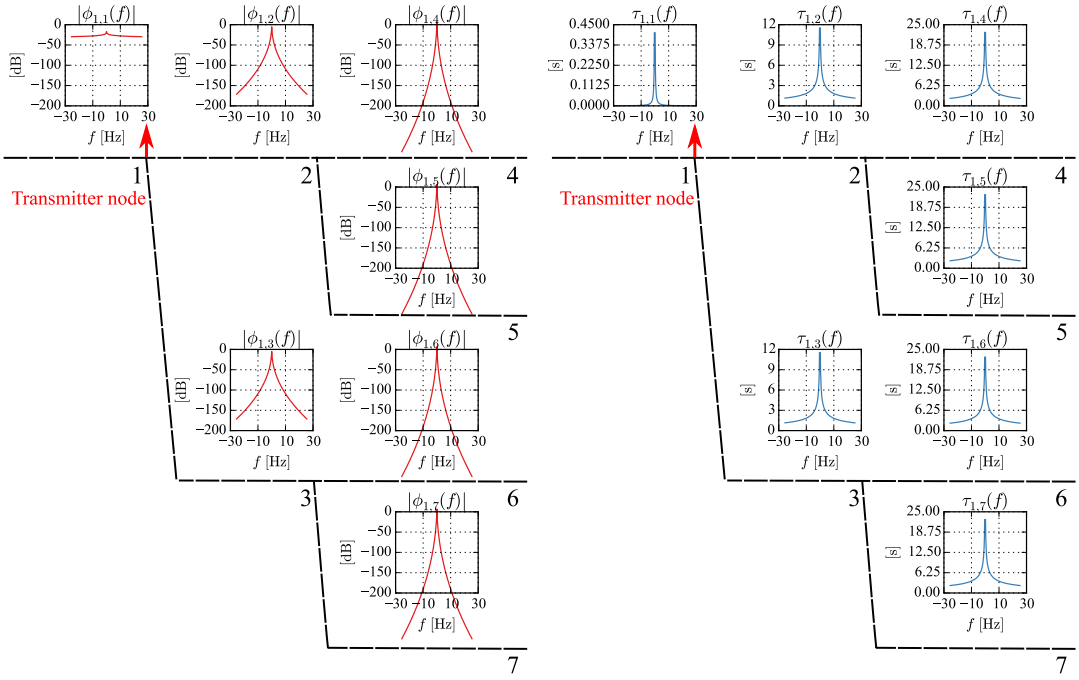

Fig. 8: Gain and group delay of node responses in a MMN at different nodes of the network, where the transmitter is located at the first bifurcation, and the receivers are located in different nodes of the MMN.

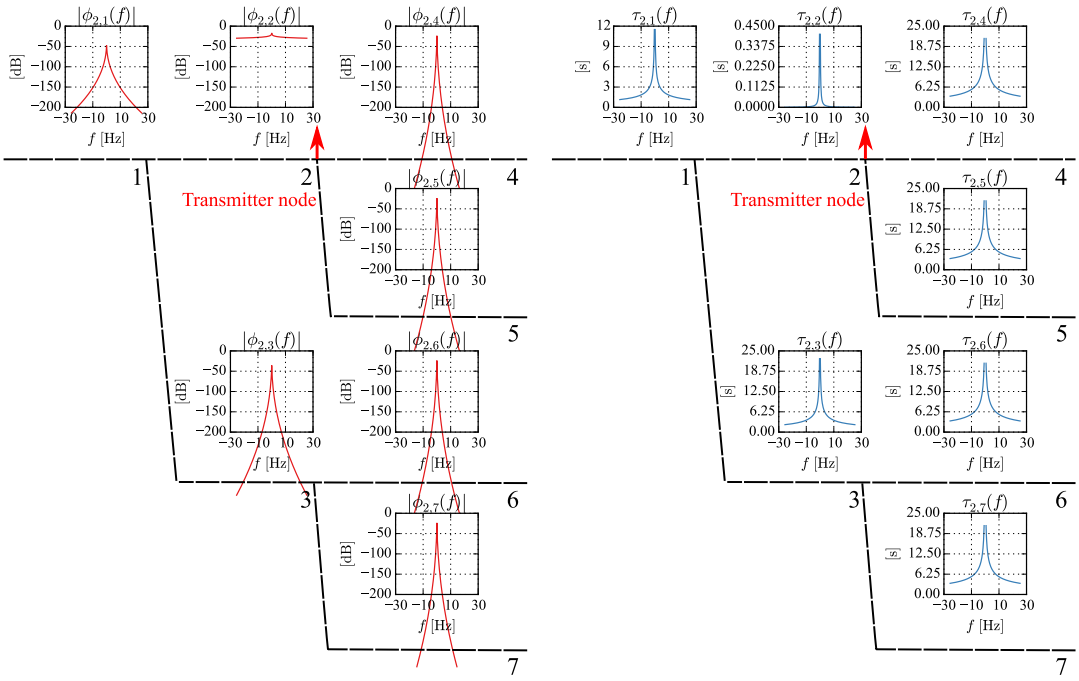

Fig. 9: Gain and group delay of node responses in a MMN at the different nodes of the network, where the transmitter is located at the second bifurcation, and the receivers are located in different nodes of the MMN.

[6] W. R. Gilks, *Markov chain monte carlo*. Wiley Online Library, 2005.

[7] D. T. Gillespie, "Stochastic simulation of chemical kinetics," *Annu. Rev. Phys. Chem.*, vol. 58, pp. 35–55, 2007.

[8] W. O. Hancock, "Bidirectional cargo transport: moving beyond tug of war," *Nature Reviews Molecular Cell Biology*, vol. 15, no. 9, pp. 615–628, 2014.

[9] N. Hirokawa, S. Niwa, and Y. Tanaka, "Molecular motors in neurons: transport mechanisms and roles in brain function, development, and disease," *Neuron*, vol. 68, no. 4, pp. 610–638, 2010.

[10] S. Hiyama, T. Inoue, T. Shima, Y. Moritani, T. Suda, and K. Sutoh, "Autonomous loading, transport, and unloading of specified cargoes by using dna hybridization and biological motor-based motility," *Small*, vol. 4, no. 4, pp. 410–415, 2008.

[11] Y.-N. Jan and L. Y. Jan, "Branching out: mechanisms of dendritic arborization," *Nature Reviews Neuroscience*, vol. 11, no. 5, pp. 316–328, 2010.

[12] C. Johnson, *Numerical solution of partial differential equations by the finite element method*. Courier Corporation, 2012.

[13] S. Klumpp, T. M. Nieuwenhuizen, and R. Lipowsky, "Self-organized density patterns of molecular motors in arrays of cytoskeletal filaments," *Biophysical journal*, vol. 88, no. 5, pp. s3118–3132, 2005.

[14] A. B. Kolomeisky and M. E. Fisher, "Molecular motors: a theorist's perspective," *Annu. Rev. Phys. Chem.*, vol. 58, pp. 675–695, 2007.

[15] Y. L. Koon, C. G. Koh, and K.-H. Chiam, "Computational modeling reveals optimal strategy for kinase transport by microtubules to nerve terminals," *PloS one*, vol. 9, no. 4, p. e92437, 2014.

[16] P. Kythe, *Greens Functions and Linear Differential Equations: Theory, Applications, and Computation*, ser. Chapman & Hall/CRC Applied Mathematics & Nonlinear Science. CRC Press, 2011.

[17] S. MacNamara, A. M. Bersani, K. Burrage, and R. B. Sidje, "Stochastic chemical kinetics and the total quasi-steady-state assumption: application to the stochastic simulation algorithm and chemical master equation," *The Journal of chemical physics*, vol. 129, no. 9, p. 095105, 2008.

[18] F. Mesiti and I. Balasingham, "Nanomachine-to-neuron communication interfaces for neuronal stimulation at nanoscale," *IEEE Journal on Selected Areas in Communications*, vol. 31, no. 12, pp. 695–704, 2013.

[19] M. J. Moore, T. Suda, and K. Oiwa, "Molecular communication: modeling noise effects on information rate," *IEEE Transactions on NanoBioscience*, vol. 8, no. 2, pp. 169–180, 2009.

[20] J. M. Newby and P. C. Bressloff, "Directed intermittent search for a hidden target on a dendritic tree," *Physical Review E*, vol. 80, no. 2, p. 021913, 2009.

[21] ——, "Quasi-steady state reduction of molecular motor-based models of directed intermittent search," *Bulletin of mathematical biology*, vol. 72, no. 7, pp. 1840–1866, 2010.

[22] T. Nitta, A. Tanahashi, M. Hirano, and H. Hess, "Simulating molecular shuttle movements: Towards computer-aided design of nanoscale transport systems," *Lab on a Chip*, vol. 6, no. 7, pp. 881–885, 2006.

[23] M. Pierobon and I. F. Akyildiz, "Capacity of a diffusion-based molecular communication system with channel memory and molecular noise," *IEEE Transactions on Information Theory*, vol. 59, no. 2, pp. 942–954, 2013.

[24] M. C. Reed, S. Venakides, and J. J. Blum, "Approximate traveling waves in linear reaction-hyperbolic equations," *SIAM Journal on Applied Mathematics*, vol. 50, no. 1, pp. 167–180, 1990.

[25] M. J. Schnitzer, K. Visscher, and S. M. Block, "Force production by single kinesin motors," *Nature cell biology*, vol. 2, no. 10, pp. 718–723, 2000.

[26] P. Sjöberg, P. Lötstedt, and J. Elf, "Fokker–planck approximation of the master equation in molecular biology," *Computing and Visualization in Science*, vol. 12, no. 1, pp. 37–50, 2009.

[27] T. Suda, M. Moore, T. Nakano, R. Egashira, A. Enomoto, S. Hiyama, and Y. Moritani, "Exploratory research on molecular communication between nanomachines," in *Genetic and Evolutionary Computation Conference (GECCO), Late Breaking Papers*, 2005, pp. 25–29.

[28] K. Visscher, M. J. Schnitzer, and S. M. Block, "Single kinesin molecules studied with a molecular force clamp," *Nature*, vol. 400, no. 6740, pp. 184–189, 1999.

Youssef Chahibi (S'13) received the Ph.D. and the M.S. degree from the Georgia Institute of Technology, Atlanta, USA, in 2012 and 2016, respectively, and the Diplôme d'Ingénieur in Telecommunications and Networks from Institut National Polytechnique de Toulouse, France, in 2011. He was a physical-layer Engineer at Alcatel-Lucent, Antwerp, Belgium, during 2011. He joined the BWN lab of the School of Electrical and Computer Engineering, Georgia Institute of Technology, Atlanta, in January 2012, supervised by Prof. Ian F. Akyildiz. During 2015, he was a fellow of the Research Council of Norway at the Norwegian University of Science and Technology (NTNU) in Trondheim, Norway, collaborating with Prof. Balasingham's Biomedical Sensor Network Research Group. His research interests include nanoscale biologically-inspired communications, nanonetworks and drug delivery systems.

Ian F. Akyildiz (M'86-SM'89-F'96) received the B.S., M.S., and Ph.D. degrees in computer engineering from the University of Erlangen-Nurnberg, Germany, in 1978, 1981, and 1984, respectively. Currently, he is the Ken Byers Chair Professor in Telecommunications with the School of Electrical and Computer Engineering, Georgia Institute of Technology, Atlanta, GA, USA, the Director of the Broadband Wireless Networking Laboratory and Chair of the Telecommunication Group at Georgia Tech. Since September 2012, Dr. Akyildiz is also a FiDiPro Professor (Finland Distinguished Professor Program (FiDiPro) supported by the Academy of Finland) at Tampere University of Technology, Department of Communications Engineering, Finland. He received numerous awards from IEEE and ACM. His current research interests are in nanonetworks, Long Term Evolution (LTE) advanced networks, cognitive radio networks, and wireless sensor networks.

Ilangko Balasingham (S'91-M'98-SM'11) received the M.S. and Ph.D. degrees in signal processing from the Department of Electronics and Telecommunications, Norwegian University of Science and Technology, Trondheim, Norway, in 1993 and 1998, respectively, and the M.S. degree from the Department of Electrical and Computer Engineering, University of California at Santa Barbara, Santa Barbara, CA, USA. Since 2002, he has been with the Intervention Center, Oslo University Hospital, Oslo, Norway, as a Senior Research Scientist, where he heads the Wireless Sensor Network Research Group. He is Professor in Signal Processing in Medical Applications at NTNU since 2006. His research interests include super-robust short range communications for both in-body and on-body sensors, body area sensor network, microwave short range sensing of vital signs, short range localization and tracking mobile sensors, and nanoneural communication networks.